Performances of SR Drive for Electrical Power Steering Systems

Jin-Woo Ahn*, Dong-Hee Lee and Young-Ju An*****

Abstract - The SRM (Switched Reluctance Motor) has a more inherent simple mechanical structure, greater ruggedness and higher efficiency than a conventional AC motor. It is for these reasons that SRM is widely applied in an extensive range of industrial applications. In this paper, SRM is designed and analyzed for EPS (Electrical Power Steering) application. Electrical power steering in a vehicle plays the role of reducing a driver's handling control power. For proper design, a FEM analysis is implemented according to the rotor structure. Using both a FEM and a magnetic circuit analysis, a designed motor is simulated and tested. The effectiveness of the suggested SRM drive for EPS application is verified by the prototype motor drive tests.

Keywords: SRM, EPS, design and analysis

1. Introduction

The SRM has a more inherent simple mechanical structure, greater ruggedness and higher efficiency than a conventional AC motor. For these reasons, the SRM is widely applied in an industrial range of industrial applications [1-4].

A conventional power steering system uses oil-pressure that is connected to a mechanical engine, having a complex housing and a tube structure. Once the engine is stopped, the oil pump and the system can no longer operate. Recently, the EPS (electrical power steering) system has been studied in great detail for high performance and environmental consideration. Because EPS uses motor power to control the direction of the wheels, the additional oil pump and complex tube structure are unnecessary, and fuel economy and acceleration capability are improved [5]. For the EPS application, high reliability and high tolerance of both motor and drive system are essential in order to endure an external impact from the road during actual driving. For these reasons, the SRM with inherent ruggedness has been studied intently for the purposes of EPS and electrical vehicle application.

This paper presents design and characteristics analysis of the SRM drive for an EPS application. A rack mounted EPS system is considered in this paper. A reduced dimension and a mechanical structure are targeted in the design stage. Under restricted design conditions, motor design parameters are determined to meet required torque and power. A 12/8 motor is selected to obtain smooth torque generation and simple circuit power system. With a CAD and a FEM for magnetic circuit analysis, a prototype motor is designed and tested. The effectiveness of the suggested SRM drive for EPS application is tested by the prototype motor drive.

* Department of Electrical and Computer Engineering, Kyungsungg University, Busan, Korea. (jwahn@ks.ac.kr)
** LG-OTIS Co., Korea. (dhlee5@hanmail.net)
*** Department of Electrical and Control Engineering Pukyong University, Busan, Korea. (anyj@pknu.ac.kr)
Received:May 7, 2003 ; Accepted: November 3, 2003

2. Rack Mounted Eps System

Power steering is used to a much greater extent in modern vehicles due to the larger size of vehicles and desire of drivers to drive more comfortably. A hydraulic power steering system requires more space and complex control, resulting in a decrease in efficiency. Pinion type power steering is easier to construct than column type. However, the torque produced in pinion type steering is low and is limited to application in small vehicles. Column type power steering for large torque and power production has been developed recently. Fig. 1 shows a conventional rack mounted power steering system. The steering power is boosted by a hydraulic system using engine power. It could be replaced by an electric system for driver's convenience and efficiency. The dotted sections, which include oil pump, pulley & belt, return and pressure line, and housing, are replaced only by electrical motor and controller. An EPS utilizes only motor power for the adjustment of wheel directions. In Fig. 1, the electrical motor can be combined with a gear box and oil pump, while the pulley and belt could be rejected as indicated by the dashed-box.

Because conventional equipment contains various restrictions, motor size is constrained and the center of a rotor's shaft must be used as a wheel shaft rod as indicated in Fig. 2. The maximum length is under 146 [mm], and the outer radius is restricted to 40.5 [mm]. The center hole of the radius, which is 20 [mm], cannot be used to house the motor.

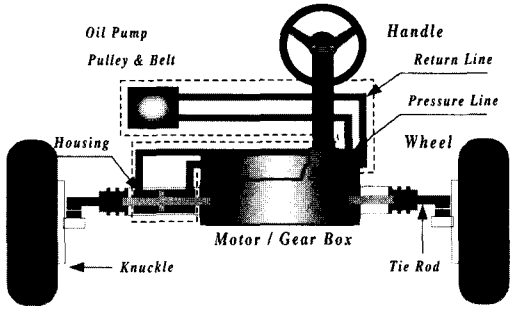

Fig. 1 Power steering system

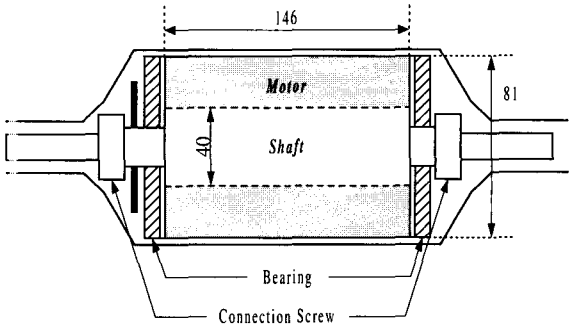

Fig. 2 Restricted motor specifications for rack mounted system

Fig. 3 shows the required performance of a motor for rack mounted EPS. The motor is supplied by a 12[V] battery.

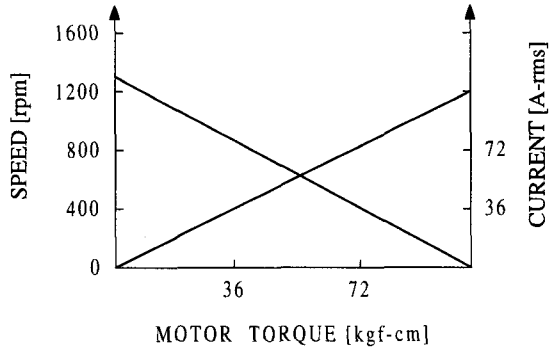

Fig. 3 Required performance of the electric motor

3. Design and Fem Analysis

3.1 Basic Design

Fig. 4 illustrates an inductance profile and a phase current in a linear analysis of the motor. The reluctance torque is produced by the square of a phase current and the gradient of inductance.

With the assumption of a square wave current in a positive torque region, the reluctance torque of the motor can be calculated as follows.

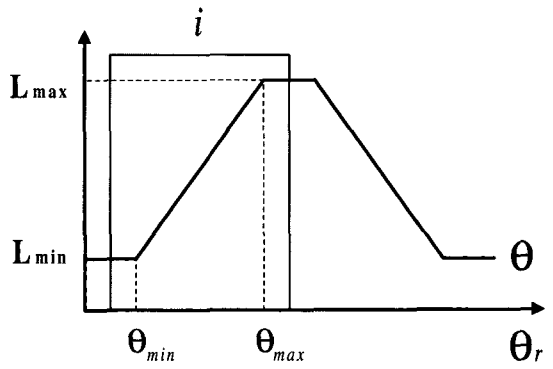

Fig. 4 The phase inductance profile and phase current

$$T_{em} = \frac{1}{2} i^2 \frac{\Delta L}{\Delta \theta} \tag{1}$$

$$\Delta L = L_{\max} - L_{\min} \tag{2}$$

$$\Delta \theta = \theta_{\max} - \theta_{\min} \tag{3}$$

where, L_{max} and L_{min} denote the maximum and minimum inductance of a phase winding, respectively. And L_{min} can be expressed by the inductance ratio K_2.

$$L_{\min} = \frac{1}{K_2} L_{\max} \tag{4}$$

The average torque of an m-phase SRM can be expressed as follows.

$$T_{ave} = \frac{m}{\theta_r} \int_0^{\theta_r} T_{em} \cdot d\theta = \frac{m}{2} \cdot \frac{(K_2 - 1) i^2}{K_2 \theta_r} \cdot L_{\max} \tag{5}$$

where, θ_r denotes rotor pole-arc. In a simple magnetic circuit, winding inductance is maximized in the aligned position of a rotor and a stator pole, and can be calculated as follows.

$$L_{\max} = \frac{1}{2} N^2 \frac{\mu_0 b l}{g} \tag{6}$$

where, μ_0 is air-gap permeability, and g is an air-gap. N denotes the turn number of a stator winding. The effective area of a linkage flux is defined as multiplication of effective width, b and core length, l of a magnetic circuit. The effective width of a magnetic circuit is determined as the minimum of stator and rotor teeth.

$$b_s = D_1 \frac{\alpha_s \pi}{N_s} \tag{7}$$

$$b_r = (D_1 - 2g)\frac{\alpha_r \pi}{N_r} \tag{8}$$

$$b = \min\{b_s, b_r\} \tag{9}$$

where, D_1 is the inner radius of the stator. And b_s and b_r are the teeth width of stator and rotor, respectively. N_s and N_r denote the number of poles of the stator and rotor, respectively. α_s and α_r are the pole-arc of stator and rotor.

In the determination of a proper stator pole arc, the slot area must be considered in the view of an effective winding area. The slot area must be wider than the effective winding area determined by a phase current, a current density and number of turns. For the proper determination of design parameters, an iterative calculation is required. Once design parameters are considered in a linear region, nonlinear analysis is executed for a superior design.

Table 1 Motor specifications

Power	320 [W]	Rated Voltage	12 [V]
Rated speed	800 [rpm]	Rated torque	3.6 [Nm]
Stack length	105 [mm]	Air gap	0.2 [mm]

3.2 Characteristic Analysis with CAD and FEM

The basic design in a linear condition makes it possible to achieve a speedy design approach, but it is impossible to analyze nonlinear characteristics. In this paper, CAD and FEM analysis are used to analyze nonlinear characteristics of the motor. With restricted design conditions on motor size and rotor yoke, a rotor and a stator pole arc are investigated for the desired output torque and speed.

Three types SRM are analyzed in the restricted motor specification as shown in Fig. 2; 6/4, 8/6 and 12/8. Fig. 5 and Fig. 6 show analysis results in each type of motor. In Fig. 5, 8/6 SRM indicates higher efficiency and output torque than that of 12/8 type in 800 [rpm].

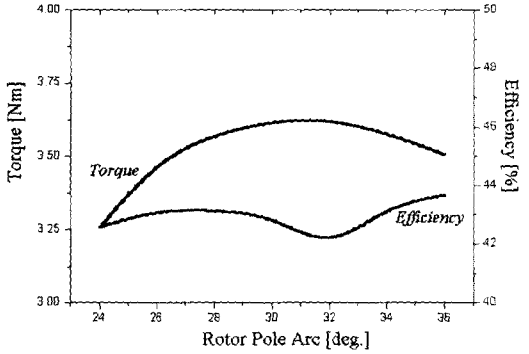

(a) 6/4 SRM (βs = 32°)

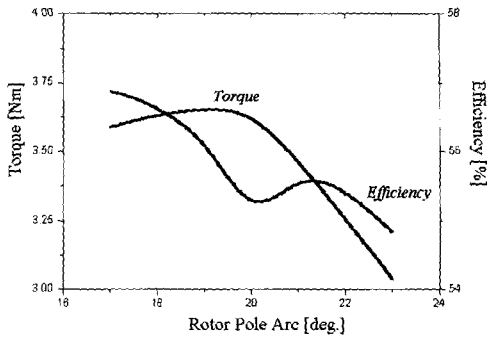

(b) 8/6 SRM (βs = 20°)

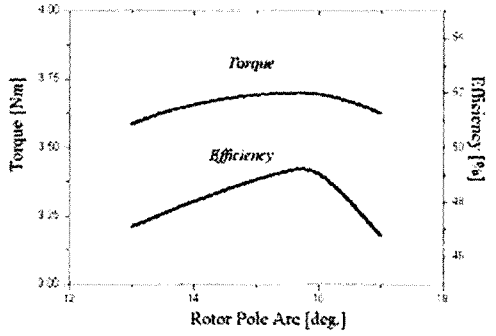

(c) 12/8 SRM (βs = 16°)

Fig. 5 Analyzed performance in 800 [rpm]

The designed motor can produce 3.6 [Nm] in 800 [rpm] as shown in Fig. 5. However, only the 12/8 motor is satisfied in the 400 [rpm] condition as shown in Fig. 6.

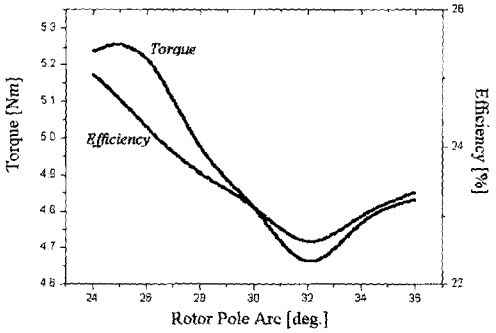

(a) 6/4 SRM (βs = 32°)

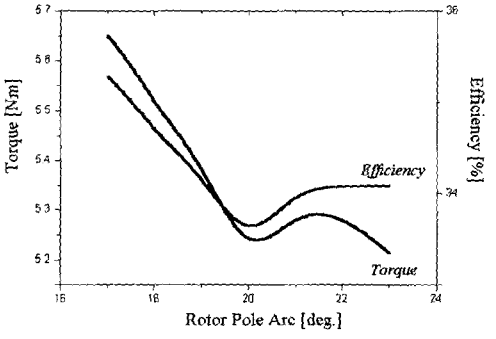

(b) 8/6 SRM (βs = 20°)

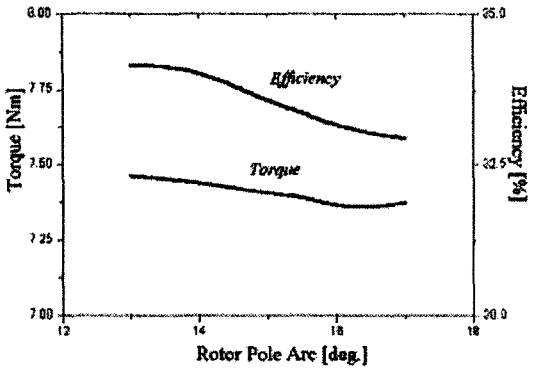

(c) 12/8 SRM ($\beta s = 16°$)

Fig. 6 Analyzed performance in 400 [rpm]

Moreover, the 8/6 motor requires more complex power conversion than that of the 12/8 motor.

Table 2 depicts the summarized analysis of the three types of motors. With consideration given to power circuit and torque ripple, the 12/8 SRM is selected in an EPS application in this paper.

Table 2 Analysis results

	6/4 SRM		8/6 SRM		12/8 SRM	
Speed [rpm]	800	400	800	400	800	400
Torque [Nm]	3.63	4.75	3.65	5.24	3.42	7.67
TF [rms]	2.03	2.60	2.16	3.13	1.18	2.02
Efficiency [%]	42.55	22.86	55.30	33.65	51.98	31.95
Turn on angle	50.0		36.0		25.0	
Turn off angle	77.0		52.0		42.0	
Dwell angle	27.0		16.0		17.0	

Table 2 and Fig. 7 show the designed motor specification and the dimension of the rotor and the stator. With the analysis results, the rotor pole arc is designed as 15.5 [deg.].

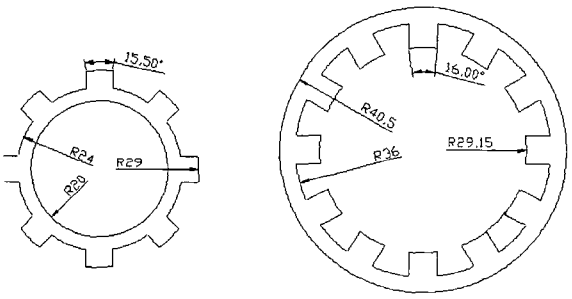

Fig. 7 Design dimension of prototype motor

Fig. 8 illustrates the flux distribution and the magnetic force direction as the result of a FEM analysis.

In the 2-D FEM analysis, the iron loss is higher in the rotor and the stator yoke than in the rotor and the stator pole. Due to restricted motor specifications, the depths of the stator and rotor yoke are limited. However, the stator and the rotor pole arc are selected for good performance.

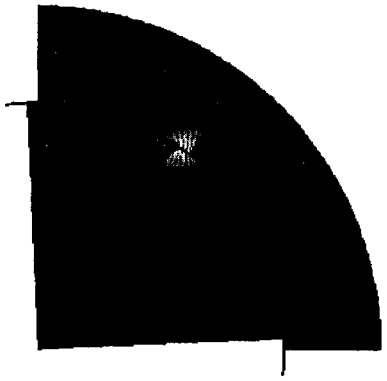

Fig. 8 Flux distribution

4. Experiments and Results

The overall control system is shown in Fig. 9. It has a motor, inverter and controller with a dynamometer system. The control block diagram is shown in Fig. 10. Torque command, phase current and encoder signal detected by a DSP based controller are used to calculate switching-on and –off angle. Phase current, speed and position signal are monitored and used for the control.

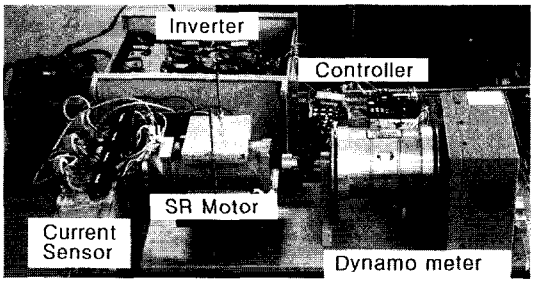

Fig. 9 Experimental set-up

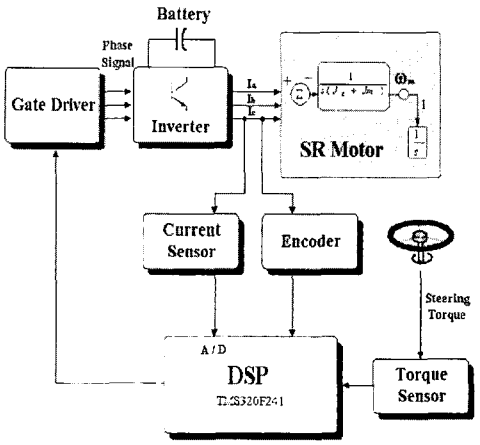

Fig. 10 Control block diagram

4.1 Motor

Fig. 11 shows the stator and rotor structure of the prototype

motor. With a given housing, a 12-pole stator with 12-turn winding is inserted. The rotor must have a hole in the rotor shaft for moving the wheel rod. An encoder is mounted in the prototype motor for the test.

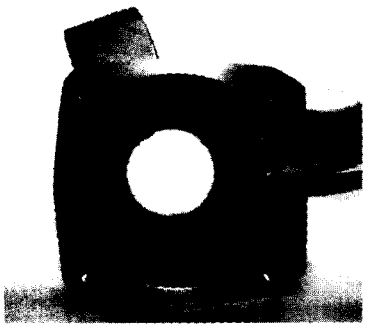

(a) stator structure

(b) rotor and shaft structure

Fig. 11 Photograph of prototype motor

4.2 Inverter

Fig. 12 shows an asymmetric inverter. This inverter has 2 switches and 2 diodes per phase and each phase can be operated independently. This type of inverter has versatile performances and high capability of current overlap during commutation. However, there are two phase switches and the voltage drop is double that of any other type. This is very disadvantageous, especially during low voltage operation. Fig. 12 (b) shows 3 modes of the inverter, magnetizing wheeling and demagnetizing mode. In mode 1, the phase current flows by turning on 2 switches of the phase. In mode 2, one switch is off while the phase current wheels though the remaining switch and wheeling diode. In mode 3, the current is returned to the source and disappears rapidly. The currents are overlapped with next phase current during the mode.

4.3. Controller

The controller adopts a TMS300F241 DSP chip, which is designed for a motor control and has some ports to detect current and encode pulses. This makes it easy to design hardware for the controller. Fig. 10 shows the complete control system. The encoder signal is isolated to the control signal via TLP181 and the power of the controller is flyback type SMPS and on the board. The over-current is detected using a resistor and cuts all the inverter signals in the control algorithm. The speed of the controller shown in Fig. 13 has a P-I controller and the output is the PWM signal.

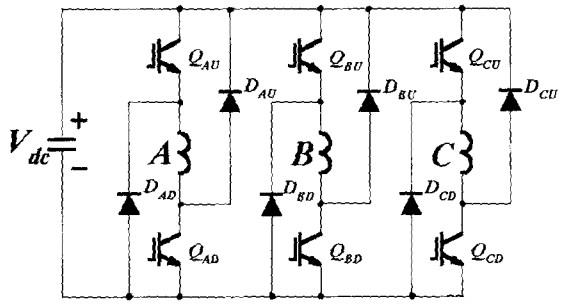

(a) Asymmetric inverter

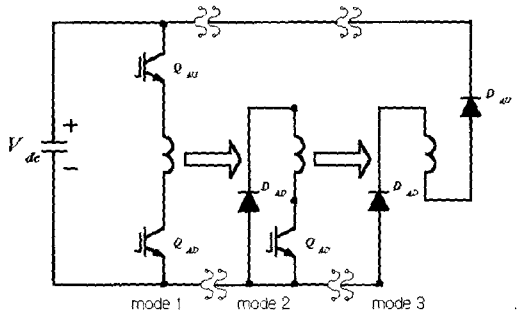

(b) Modes in the excitation control

Fig. 12 Inverter and modes

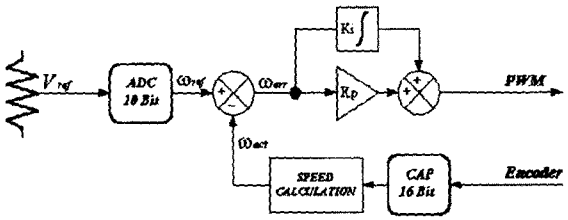

Fig. 13 Speed controller

4.4 Results and discussions

The performances are tested using a prototype drive system. Fig. 14 details currents according to a turn-on angle with the fixing turn-off angle of 20° at 800rpm. The phase angle for a flat-top current is built at about 6 [deg.] of the turn-on angle. Fig. 15 shows measured torque-speed characteristics. The torque meets the requirement but efficiency is somewhat low. This is due to the fact that the dimensions are restricted and that they are for a magnetic type motor. This could be overcome using high permeability steel and modifying dimensional restrictions. A speed response is tested and shown in Fig. 16. The speed response is 0.2 [sec] from 0 to 800rpm and it is within the specifications.

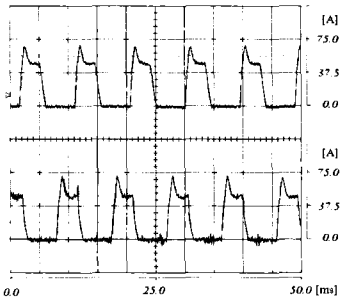

(a) Turn-on angle = 2.8°

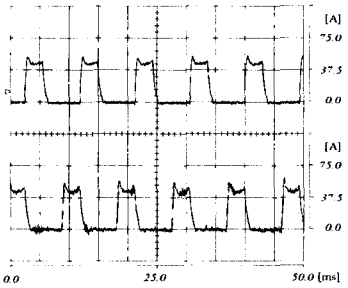

(b) Turn-on angle = 5.27°

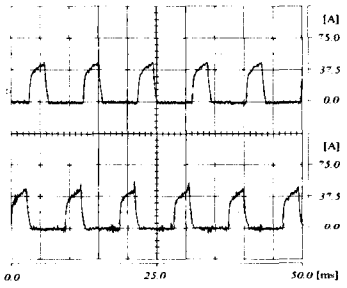

(c) Turn-on angle = 7.38°

Fig. 14 Current waveforms according to turn-on angle

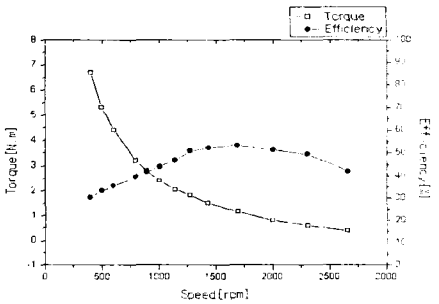

Fig. 15 Speed – torque characteristics of proto-type motor

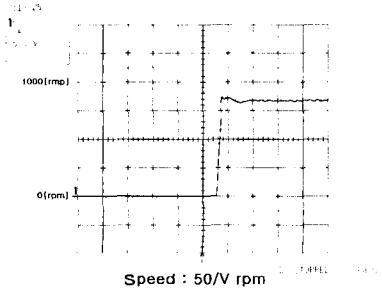

Fig. 16 Speed response

5. Conclusions

This paper presents design and characteristics analysis of the SRM drive for EPS application. The rack mounted EPS system is considered in this paper. With restricted dimensions and mechanical structure, three general types of SRM are analyzed to meet the performance requirements.

For a smooth torque generation and a simple circuit power system, a 12/8 motor is selected with analyzed results. With FEM and magnetic circuit analysis, the prototype motor is simulated and tested. In the FEM and experimental results, designed SRM satisfies both torque and speed requirements. Nevertheless, the drive efficiency can be improved with design modifications.

References

[1] Aly Badawy, Jeff Zuraski, Farhad Bolourchi and Ashok Chandy, "Modeling and Analysis of an Electric Power Steering System" Steering and Suspension Technology Symposium, 1999.

[2] Aly A. Badawy, Farhad Boloruchi, Steven K. Gaut, "E-Steer ™ Redefines Steering Technology", Automotive Engineering, Automotive Systems Review of Technical Achievements, pp. 15-18, SAE International Magazine, September 1997.

[3] Jin-Woo Ahn, Switched Reluctance Motor, O-Sung Media, 2001.

[4] Texas Instruments "TMS320F243/F241/C242 DSP Control ers Reference Guide - System and Peripherals", January 2000.

[5] Jin-Woo Ahn, *Switched Reluctance Motor*, O-Sung Media, 2001.

[6] S. Y. Pyo and J. W. Ahn, "High Efficiency PLL Control for SRM Drive", The Journal of Electronics, KIPE, Vol. 5, No. 3, pp. 215-220, 2000.

[7] C. S. Kim, M. G. Kim, H. G. Lee and J. W. Ahn, "Development of SRM and Drive System for Small Pallet Truck" Annual Proc. of KIEE, pp. 732-734, 2000.

[8] C. S. Kim, S. G. Oh, J. W. Ahn and Y. M. Hwang, "The Design and the Characteristics of SRM Drive for Low Speed Vehicle" Annual Proc. of KIEE, pp. 871-873, 2001.

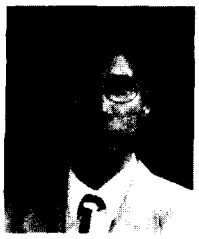

Jin-Woo Ahn

He was born in Busan, Korea, in 1958. He received the B.S., M.S., and Ph.D. degree in Electrical Eengineering from Pusan National University, Busan, Korea, in 1984, 1986, and 1992, respectively.

He has been with Kyungsung University, Busan, Korea, as a professor in the Department of Electrical and Computer Engineering since 1992. He was a Visiting Professor in the Dept. of EE, Glasgow University, U.K 1995 and UW-Madison, USA 1998, respectively. He is the author of several books and has several patents about SR motor and the author of more than 100 papers. His current research interests are motor drive system and electric vehicle drive. He awarded several prizes including best paper in 2002, academic achievement prize in 2003 from Korean Institute of Electrical Engineers and academic achievement prize in 2003 from Korean Institute of Power Electronics, and best paper prize in 2003 from The Korean Federation of Science and Technology Societies, respectively. He is an editorial director of KIEE Society of Electrical Machinery and Energy Conversion and an academic director of Korean Institute of Power Electronics.

Dr. Ahn is a life member of Korean Institute of Electrical Engineers, a member of Korean Institute of Power Electronics and a senior member of IEEE.

Tel : +82-51-620-4773

Dong-Hee Lee

He was born in Nov. 11, 1970 and received the B.S, M.E, and Ph. D. degrees in electrical engineering at Pusan National University, respectively. Major research field is about motor drive system and micro-process application. He is a member of KIEE and currently working as senior researcher at OTIS-LG.

Tel : +82-51-522-1503

Young-Joo An

He was born in Jan. 22, 1957 and received the B.S. degrees in electrical engineering at Pusan National University Technology, and M.E, and Ph. D. degrees in electrical engineering at Pusan National University, respectively. Major research field is about motor drive and control. He is a member of KIEE and with Dept. of Electrical and Control as an associate professor.

Tel : +82-51-620-1638